



Get Clarity On Generics

Cost-Effective CT & MRI Contrast Agents



FRESENIUS
KABI

WATCH VIDEO

AJNR




This information is current as
of August 7, 2025.

Dual-Energy CTA Iodine Map Reconstructions Improve Visualization of Residual Cerebral Aneurysms following Endovascular Coiling

Dylan N. Wolman, Gabriella Kuraitis, Eric Sussman,
Benjamin Pulli, Anke Wouters, Jia Wang, Adam Wang,
Maarten G. Lansberg and Jeremy J. Heit

AJNR Am J Neuroradiol published online 1 August 2024
<http://www.ajnr.org/content/early/2024/08/01/ajnr.A8305>

Dual-Energy CTA Iodine Map Reconstructions Improve Visualization of Residual Cerebral Aneurysms following Endovascular Coiling

 Dylan N. Wolman, Gabriella Kuraitis, Eric Sussman, Benjamin Pulli, Anke Wouters, Jia Wang, Adam Wang,  Maarten G. Lansberg, and  Jeremy J. Heit



ABSTRACT

BACKGROUND AND PURPOSE: Material-specific reconstructions of dual-energy CTA (DECTA) can highlight iodinated contrast, subtract predefined materials, and reduce metal artifact. We present a technique to improve detection of residual aneurysms after endovascular coiling by which iodine-map DECTA (IM-DECTA) reconstructions subtract platinum coil artifacts in MIP images (MIP IM-DECTA) and assess if IM-DECTA offers improved detection over conventional CTA (CCTA) or monoenergetic DECTA.

MATERIALS AND METHODS: We included consecutive patients who underwent endovascular aneurysm coiling with follow-up DECTA and DSA within 24 months. DECTA was performed at 80- and 150-kVp tube voltages on a rapid kV-switching single-source Revolution scanner. CCTA and IM-DECTA series were reconstructed. Reference-standard DSA was compared with CCTA, 50- and 70-keV virtual monochromatic DECTA, IM-DECTA, and MIP IM-DECTA. Blinded to DSA data, cross-section images were reviewed in consensus by 3 neurointerventionalists for residual aneurysms and assigned modified Raymond-Roy classifications (mRRC). Sensitivity, specificity, and accuracy of each series is reported relative to DSA, and single-factor ANOVA and pair-wise Spearman correlation coefficients compared the accuracy of each series. Readers provided ROI measurements of HU deviation adjacent to the aneurysm neck for quantitative noise assessment and qualitatively scored each series on a 3-point Likert-style scale ranging from uninterpretable to excellent image quality.

RESULTS: Twenty-one patients with 25 coiled aneurysms were included. Mean time from DECTA to DSA was 286 ± 212 days. IM-DECTA and MIP IM-DECTA most sensitively (89% and 90%) and specifically (93% and 93%) detected residual aneurysms relative to CCTA (6% and 86%). Relative to DSA, IM-DECTA and MIP IM-DECTA most accurately detected (92% versus 28% for CCTA) and classified residual aneurysms by mRRC ($\rho_{\text{C-CTA}} = -0.08$; $\rho_{\text{IM}} = 0.50$; $\rho_{\text{IM-MIP}} = 0.55$; $P < .001$). Reader consensus reported the best image quality at the aneurysm neck with IM-DECTA and MIP IM-DECTA, with 56% of CCTAs considered uninterpretable versus 0% of IM-DECTAs, and image noise was significantly lower for IM-DECTA (27.9 ± 3.6 HU) or MIP IM-DECTA (26.8 ± 3.5 HU) than CCTA (103.2 ± 13.3 HU; $P < .001$).

CONCLUSIONS: MIP IM-DECTA can subtract coil mass artifact and is more sensitive and specific than CCTA for the detection of residual aneurysms after endovascular coiling.

ABBREVIATIONS: CCTA = conventional CTA; DECT = dual-energy CT; DECTA = dual-energy CTA; IM = iodine map; mRRC = modified Raymond-Roy classification

CT angiography is a ubiquitous standard for the noninvasive evaluation of the craniocervical vasculature. However, the utility of CTA for the evaluation of residual or recurrent aneurysms after endovascular coil embolization is limited by beam-hardening artifact resultant primarily from selective low-energy

photon absorption by the high atomic weight platinum coil mass.^{1,2} MRA is the current standard of care in aneurysm follow-up but may similarly offer limited evaluation of the treated aneurysm and adjacent parent vessel due to susceptibility artifact from the coil mass, with reduced availability, higher costs, and inferior spatial resolution as compared with CTA, with particularly reduced sensitivity for small residual aneurysms.³ DSA

Received February 19, 2024; accepted after revision April 1.

From the Department of Diagnostic Imaging (D.N.W.), The Warren Alpert School of Medicine at Brown University, Rhode Island Hospital, Providence, Rhode Island; Department of Radiology (G.K., B.P., A.Wouters, J.W., A.Wang, J.J.H.), Neuroimaging and Neurointervention Section, and Department of Neurology (M.G.L.), Stanford University Hospital, Palo Alto, California; and Department of Neurosurgery (E.S.), Hartford Hospital, Ayer Neuroscience Institute, Hartford, Connecticut.

Please address correspondence to Dylan N. Wolman, MD, 110 Lockwood St, APC Suite 701, Providence, RI 02903; e-mail: dylan_wolman@brown.edu; @dylanwolman

 Indicates article with online supplemental data.

<http://dx.doi.org/10.3174/ajnr.A8305>

SUMMARY

PREVIOUS LITERATURE: The use of IM-DECTA has not been evaluated for the detection and characterization of residual aneurysms after coil embolization. Previous studies have primarily examined the use of metal-artifact reduction software and virtual monoenergetic reconstructions to reduce clip and coil associated beam-hardening artifact following aneurysm treatment, but beam-hardening artifact significantly limited the detection of residual aneurysms.

KEY FINDINGS: We demonstrate that IM-DECTA and MIP IM-DECTA leverage a unique reconstruction artifact to subtract platinum-associated coil mass. We found that the detection and characterization of residual aneurysms are significantly more accurate for IM-DECTA than CCTA or virtual monoenergetic reconstructions, and image noise is significantly reduced with IM-DECTA.

KNOWLEDGE ADVANCEMENT: IM-DECTA may be a viable method for the noninvasive follow-up of coiled intracranial aneurysms and may serve as a proof-of-concept for the generation of metal-specific multispectral CT reconstructions to follow-up endovascularly or surgically treated aneurysms. Further comparison against MRA and in a larger population is warranted.

remains the criterion standard for the assessment of residual or recurrent aneurysms after endovascular or surgical treatment but is a costly and invasive procedure with low but notable risks. Therefore DSA is best reserved for definitive assessment of abnormalities on noninvasive imaging or for preprocedural planning.⁴

Dual-energy CT angiography (DECTA) may leverage the improved intravascular contrast attenuation of low-energy acquisitions and reduced beam hardening artifacts of high-energy acquisitions to improve raw arterial visualization. Several studies have leveraged higher-energy virtual monoenergetic reconstructions of DECTA to improve arterial visualization and reduce beam-hardening artifact after endovascular or surgical aneurysm treatment with variable results, particularly for aneurysms treated by coil embolization.^{1,5-7} Dual-energy CT (DECT) DECT allows for spectral separation of materials with differing atomic numbers and corresponding differential attenuation of high- and low-energy photons, allowing estimation of the relative concentration of a given material within each voxel. Material-specific maps may then be generated based upon the calculated relative HU contribution of a specific material basis pair for any given voxel, subtracting the attenuation attributed to beam absorption from other materials within each voxel.⁸ For example, given a material basis pair of iodine and water, all attenuation within a given voxel is assumed to be derived from brain matter (or fat), iodine, and water, and based upon defined attenuation spectra of each material at high- and low-beam energies, subtraction of the assumed attenuation contributed by either water or iodine generates high-contrast and material-specific images, such as iodine or water maps, respectively.^{2,9} Iodine map images may improve the contrast-to-noise ratio of CTA by 40%–59% relative to conventional CTA (CCTA) while maintaining beam-hardening artifact reduction benefits.^{10,11}

We hypothesized that iodine-map (IM)-DECTA images may significantly reduce image noise and improve visualization of both the parent vessel and treated intracranial aneurysm after endovascular coiling due to both a reduction in beam-hardening artifact and the improved contrast attenuation afforded by iodine-specific image reconstructions assessed relative to CCTA and virtual monochromatic 50-keV and 70-keV DECTA images,

which have also been reported to improve iodine contrast-resolution and reduce beam hardening artifacts.¹² In addition, we leveraged a unique artifact from the generation of subtraction-based IM-DECTA images wherein platinum coils appear as dark subtraction voids, further hypothesizing that generation of MIP IM-DECTA images may effectively “subtract” the visualized coil mass. Therefore, we sought to determine if the generation of maximum intensity projection IM-DECTA (MIP IM-DECTA) images could further improve visualization of residual or recurrent aneurysms after coil embolization.

MATERIALS AND METHODS

Patients

We performed a retrospective cohort review of consecutive patients from January 2020 through December 2020 who underwent coil embolization of intracranial aneurysms and received routine follow-up DSA and DECTA within 24 months of treatment. The intended follow-up protocol was to undergo DECTA at 6–12 months posttreatment and subsequent DSA within 6–12 months posttreatment. This study was approved by our institutional review board and complied with the Health Insurance Portability and Accountability Act.

The primary outcome measures were the accurate detection of residual aneurysms and accurate assessment of the extent of aneurysm occlusion (codified by the modified Raymond-Roy classification [mRRC]) on CTA relative to reference DSA. Secondary outcome measures were the quantitative and qualitative assessments of image noise on each CTA series at the expected location of the aneurysm neck within the parent vessel to determine which series is least affected by beam-hardening artifact adjacent to coil masses. Residual aneurysms were additionally stratified by size and ratio of maximum coil mass to residual aneurysm diameter and a subgroup analysis was performed to determine if these values had an effect on aneurysm detection.

Inclusion criteria were: any patient age >18 years who underwent endovascular aneurysm coiling with or without assistive devices (including stent placement per treating physician preference) and follow-up DSA and DECTA within 24 months of initial treatment without intervening re-treatment. Patients who underwent treatment for either ruptured or unruptured aneurysms were included.

Exclusion criteria included technical failure of DECTA or postprocessing, excessive motion artifact, follow-up imaging performed <5 months from initial treatment, and retreatment of the initial aneurysm within the follow-up period.

Imaging Technical Details

All patients underwent DECTA on a fast kV-switching single-source Revolution CT scanner with a single-layer gemstone spectral imaging detector (GE Healthcare). The DECTA protocol included a noncontrast head CT and helical CT angiography of the head. Scan parameters were: rapid-switching of tube voltages between 80-kVp and 140-kVp, tube currents of 280 mAs, pitch 0.516, beam collimation of 40×0.6 mm, rotation time of 0.5 seconds, matrix size of 512×512 , section thickness of 0.625 mm, and fixed dose of 30.08 mGy CT dose index volume. Iodinated contrast was administered at a volume of 1.0 mL/kg of body weight and a maximum injection rate of 8 mL/s. Bolus tracking software was used to determine patient-specific acquisition timing, with HU-based triggering within the thoracic aorta at the level of the carina. Images were automatically reconstructed by using Xstream software (GE Healthcare) and conventional-appearing 120-kVp weighted (CCTA), virtual monochromatic 50-keV and 70-keV DECTA, and IM-DECTA images were sent to a PACS for routine interpretation. IM-DECTA images were generated by using vendor default software parameters and material basis pairs of iodine and water, with standard image outputs reflecting attenuation in HU rather than iodine concentration.

All follow-up DSAs included conventional angiographic views and dedicated orthogonal magnified oblique projections demonstrating the aneurysm neck and mimicking the working projections obtained at the time of endovascular treatment. 3D rotational angiography was performed as needed to obtain such views.

Imaging Analysis

All neuroimaging data were anonymized and placed into an OsiriX (Pixmeo) database for subsequent analyses. All imaging analyses were performed by readers who were blinded to initial and follow-up DSA data. Three readers (an experienced neurointerventional radiologist, a dual-trained neurointerventional surgeon, and a senior neurointerventional radiology fellow) were provided with source 0.625-mm axial CCTA, virtual monochromatic 50-keV and 70-keV DECTA, IM-DECTA, and MIP IM-DECTA images, with MIP thickness set to default at 5 mm, but adjustable to reader preference from 2–20 mm. Readers could freely set window width and level during analysis. For the provision of MIP IM-DECTA scores, readers were instructed to adjust MIP thickness on IM-DECTA reconstructions to the point at which the coil mass was no longer visible at the level of the parent vessel. Readers were able to reconstruct coronal, sagittal, and multiplanar reformats for scoring of all CTA images.

Reader scores were collated for binary ability to visualize the aneurysm neck and mRRC per aneurysm, and reader disagreements were resolved by consensus.¹³ Reader scores were compared against criterion-standard DSA data regarding aneurysm

occlusion, with reference mRRC scores provided by a separate neurointerventional radiologist. The mRRC score was defined as follows: 1) no residual opacified aneurysm; 2) residual neck opacification only; 3a) residual aneurysm opacification within the coil interstices; and 3b) residual aneurysm opacification outside the coil interstices. Maximum residual aneurysm sizes and per-aneurysm ratios of maximal coil diameter to maximal residual aneurysm diameter (coil-to-aneurysm size ratio) were recorded from source DSA data. For cases in which readers failed to accurately classify the presence or absence of a residual aneurysm, these values were referenced to determine if residual aneurysm size or coil-to-aneurysm ratio may have influenced reader accuracy on IM-DECTA series.

Image quality was assessed qualitatively on a consensus 3-point Likert-style scale for overall interpretability of the CTA adjacent to the coil mass, with the range including uninterpretable (IQ1; defined as no ability to visualize the aneurysm neck or adjacent parent vessel due to beam-hardening artifact), moderately artifact degraded (IQ2; defined as having limited but retained visualization of the parent vessel and at least a portion of the expected location of the aneurysm neck), and excellent (IQ3; defined as having mild to no significant beam-hardening artifact obscuring the parent vessel or aneurysm neck).

Additionally, image quality was assessed quantitatively by measurements of image noise, represented through ROI measurements of HU variability placed by each reader at the parent vessel adjacent to the treated aneurysm and at the expected location of the aneurysm neck, with greater deviation values reflecting greater beam-hardening artifact effects. Mean HU ROI deviation values were calculated from each reader's ROI outputs directly and expressed as the mean standard deviation \pm standard error of the mean (SEM) to reflect the degree of local image noise with higher values reflecting greater HU variation and therefore beam-hardening artifact.¹⁴ All ROIs were confirmed by a separate reader for appropriate and concordant placement before analysis.

Statistical Analysis

For the assessment of residual aneurysm detection, the sensitivity, specificity, and accuracy of binary consensus reader scores for each CTA series is reported relative to the criterion standard DSA, and the Wilcoxon-signed rank test was reported for pair-wise comparisons of each aneurysm relative to reference standard DSA (with *P* values > .05 reflecting significantly greater agreement with the reference standard). For the scoring of aneurysm occlusion, Friedman 2-way ANOVA test and pair-wise Spearman correlation coefficients were calculated to compare the consensus ordinal scores for each aneurysm in each CTA series relative to the criterion standard mRRC derived from DSA data. Mean residual aneurysm sizes and coil-to-aneurysm size ratios, grouped by cases in which a residual aneurysm was accurately or inaccurately detected, were compared by using the Welch *t* test. Interreader agreement for residual aneurysm classification by mRRC was assessed by using the Cohen κ test.

For the quantitative assessment of image noise, the mean HU values for each CTA series were compared in a pair-wise fashion by using the 2-sample Student *t* test and by using a 1-way

Table 1: Baseline aneurysm characteristics

Aneurysm location	
Anterior communicating artery	6/25 (24%)
Posterior communicating artery	3/25 (12%)
Supraclinoid internal carotid artery	5/25 (20%)
Middle cerebral artery bifurcation	3/25 (12%)
Basilar apex	4/25 (16%)
Proximal vertebrobasilar system	4/25 (16%)
Ruptured on presentation	22/25 (88%)
Mean aneurysm size (maximal diameter)	6.3 ± 3.9 mm (2–17 mm)
Mean residual aneurysm size (maximal diameter)	2.7 ± 1.1 mm (1.4–5.4 mm)
Mean coil mass size (maximal diameter)	6.6 ± 2.7 mm (2.7–14 mm)
Mean coil-to-aneurysm size ratio	3.0 ± 1.4 (1.6–5.3)
Mean time from DECTA to follow-up DSA	286 ± 212 days (22–683 days)
Follow-up DSA mRRC	
mRRC 1	14/25 (56%)
mRRC 2	3/25 (12%)
mRRC 3a	5/25 (20%)
mRRC 3b	3/25 (12%)

Note:—Summary of baseline aneurysm characteristics. Mean aneurysm size is derived from initial DSA and mean residual aneurysm size and coil-to-aneurysm size ratio is derived from follow-up DSA. Mean coil mass size is derived from bone kernel noncontrast head CT images. Sizes are expressed as mean ± SD (range) in mm.

ANOVA test across all series. Qualitative assessments of image noise were assessed by a 3-point Likert-style scale for scan interpretability for each independent aneurysm. Likert-style responses were expressed as the mode per CTA series and as consensus scores, and each series was compared by using the Kruskal-Wallis test. Interreader agreement was then assessed by using the Cohen κ test.

All data were collated in Excel (Microsoft) and statistical analyses were performed in StataIC (StataCorp). Statistical significance was set at $\alpha = .05$.

RESULTS

Baseline Aneurysm Characteristics

A total of 21 patients were included with 25 separate aneurysms. Twenty (80%) aneurysms were treated by primary coil embolization and 5 (20%) were treated by stent-assisted coiling. Most of the treated patients presented with ruptured aneurysms (22/25 [88%]). No hemorrhagic or ischemic complications occurred during treatment, and on completion angiography there was no coil herniation within the parent vessel for any treated aneurysm. Aneurysm locations were as follows: 6/25 (24%) at the anterior communicating artery; 3/25 (12%) at the posterior communicating artery; 5/25 (20%) within the supraclinoid internal carotid artery (including superior hypophyseal, paraophthalmic, carotid cave, or ventral internal carotid artery aneurysms); 3/25 (12%) at the middle cerebral artery bifurcation; 4/25 (16%) at the basilar apex; and 4/25 (16%) within the proximal vertebrobasilar system, including posterior and anterior inferior cerebellar artery and intradural vertebral artery aneurysms (Table 1).

The mean time from DECTA to follow-up DSA was 286 ± 212 days. The mean aneurysm size on pretreatment angiography was 6.3 ± 3.9 mm, with a range of 2–17 mm as measured by maximal aneurysm diameter. The mean coil mass size, as measured on bone kernel noncontrast CT head images, was 6.6 ± 2.7 mm, with a range of 2.7–14 mm as measured by average 3D diameter, or 2–17 mm as measured by maximal 2D diameter. The mean

maximal residual aneurysm diameter was 2.7 ± 1.1 mm (range 1.4–5.4 mm) and the mean coil-to-aneurysm size ratio was 3.0 ± 1.4 (range 1.6–5.3; Table 1).

Detection of Aneurysm Occlusion Characteristics

Eleven of the 25 (44%) included aneurysms demonstrated residual aneurysm opacification on follow-up DSA. These were subclassified by mRRC as follows: mRRC 1 (14/25 [56%]); mRRC 2 (3/25 [12%]); mRRC 3a (5/25 [20%]); and mRRC 3b (3/25 [12%]). Baseline residual aneurysms are reported in Table 1. Relative to reference standard DSA, IM-DECTA and MIP IM-DECTA were the overall most sensitive (75% and 83%), specific (93% and 92%), and accurate

(85% and 88%) series with superior reader agreement ($\rho_{\text{IM-DECTA}} = 0.51$, $P = .31$ and $\rho_{\text{MIP IM-DECTA}} = 0.51$, $P = .97$) as compared with CCTA, which was the least sensitive (0%), specific (86%), and accurate (23%) of all the CTA series ($\rho_{\text{CCTA}} = -0.18$, $P < .01$). Virtual monochromatic reconstructions at 50-keV and 70-keV demonstrated superior sensitivity (31% and 20%), specificity (88% and 100%), and accuracy (52% and 52%) over CCTA but remained insensitive and discordant with the reference DSA ($\rho_{50\text{keV}} = 0.33$, $P < .01$; $\rho_{70\text{keV}} = 0.41$, $P < .01$). Please note that given comparisons against reference DSAs, P values of $> .05$ indicate significant agreement with the criterion-standard. The mean size and coil-to-aneurysm size ratio of residual aneurysms missed by readers on IM-DECTA was 1.6 ± 0.2 mm and 5.1 ± 0.2, respectively, differing significantly from the mean size (3.0 ± 1.1 mm) and ratio (2.5 ± 0.9) of those accurately detected by readers ($P < .01$).

Using the mRRC, readers more accurately classified the extent of residual aneurysms on IM-DECTA ($\rho_{\text{IM-DECTA}} = 0.58$; $P = .09$) and MIP IM-DECTA ($\rho_{\text{MIP IM-DECTA}} = 0.67$; $P = .93$) series than by using CCTA ($\rho_{\text{CCTA}} = -0.04$; $P < .01$), 50-keV ($\rho_{50\text{keV}} = 0.58$; $P < .01$) or 70-keV ($\rho_{70\text{keV}} = 0.50$; $P < .01$) series. Similarly, reader classification of residual aneurysms demonstrated the greatest interreader agreement by using the IM-DECTA ($\kappa_{\text{IM-DECTA}} = 0.55$) and MIP IM-DECTA ($\kappa_{\text{MIP IM-DECTA}} = 0.58$) series when compared against CCTA ($\kappa_{\text{CCTA}} = 0.34$), 50-keV ($\kappa_{50\text{keV}} = 0.34$) or 70-keV ($\kappa_{70\text{keV}} = 0.44$) series. These associations are summarized in Table 2 and Table 3. A case example highlighting the difference in aneurysm detection between CCTA, IM-DECTA, and MIP IM-DECTA with comparison against the reference standard DSA is provided in Fig 1.

Image Noise Analysis

Quantitative image noise analyses are summarized in Table 4 and example reader prescribed ROIs are provided in the Online Supplemental Data. The mean HU standard deviation of ROIs provided for each series demonstrates the lowest image noise for IM-DECTA (27.9 ± 3.6 HU) and MIP IM-DECTA (26.8 ±

3.5 HU) series ($P < .01$) when as compared with the reference CCTA series (103.2 ± 13.3 HU; Table 4). Monochromatic CTA reconstructions at 50-keV numerically demonstrated lesser image noise relative to CCTA (78.1 ± 10.1 HU versus 103.2 ± 13.3 HU; $P = .06$) while the 70-keV series demonstrated incrementally increased image noise (129.6 ± 16.7 HU versus 103.2 ± 13.3 HU; $P = .07$; Table 4).

Table 2: Detection of residual aneurysms

	Binary Residual Aneurysm Detection				
	Sensitivity	Specificity	Accuracy	Agreement	P-Value
CCTA	0%	86%	23%	-0.18	<.01
50-keV CTA	31%	88%	52%	0.33	<.01
70-keV CTA	20%	100%	52%	0.41	<.01
IM-DECTA	75%	93%	85%	0.51	.31
MIP IM-DECTA	83%	92%	88%	0.51	.97

Note:—Sensitivity, specificity, accuracy, and reader agreement (expressed as the Pearson correlation coefficient) for residual aneurysm detection is expressed relative to reference DSA, therefore nonsignificant P -values indicate greater agreement with the reference standard.

Table 3: Residual aneurysm occlusion classification

	Agreement with mRRC by DSA		
	Pearson Correlation	κ Agreement	P-Value
CCTA	-0.04	0.34	<.01
50-keV CTA	0.58	0.34	<.01
70-keV CTA	0.5	0.44	<.01
IM-DECTA	0.58	0.55	.09
MIP IM-DECTA	0.67	0.58	.93

Note:—Pearson correlation coefficient and κ interreader variability for mRRC scoring is expressed relative to reference DSA, therefore nonsignificant P -values indicate greater agreement with the reference standard.

Qualitative analyses of image noise are summarized in Table 5. Reader consensus reported that 14/25 (56%) CCTA images were uninterpretable (IQ1) and 0/25 (0%) were of excellent image quality (IQ3). Readers reported image quality improved with 50-keV (3/25 [12%] IQ1 and 6/25 [24%] IQ3) and 70-keV (5/25 [20%] IQ1 and 4/25 [16%] IQ3) monochromatic CTA reconstructions, but reported the highest quality with review of IM-DECTA (0/25 [0%] IQ1 and 17/25 [68%] IQ3; $P < .01$) and MIP IM-DECTA series (0/25 [0%] IQ1 and 19/25 [76%] IQ3; $P < .01$). Interreader agreement of image noise was lowest with monochromatic reconstructions ($\kappa_{50\text{keV}} = 0.23$; $\kappa_{70\text{keV}} = 0.27$), intermediate with CCTA ($\kappa_{\text{CCTA}} = 0.34$), and greatest with IM-DECTA ($\kappa_{\text{IM-DECTA}} = 0.49$) and MIP IM-DECTA series ($\kappa_{\text{MIP IM-DECTA}} = 0.58$). Readers reported adequate aneurysm neck visualization most frequently with IM-DECTA and MIP IM-DECTA series (24/25 [96%]) as compared with monochromatic 50-keV (18/25 [72%]) and 70-keV (20/25 [80%]) series or CCTA (11/25 [44%]; $P < .01$). The 1 case for which the aneurysm neck was not considered visible on any series was that of the largest aneurysm, with a coil mass measuring up to 17 mm in diameter.

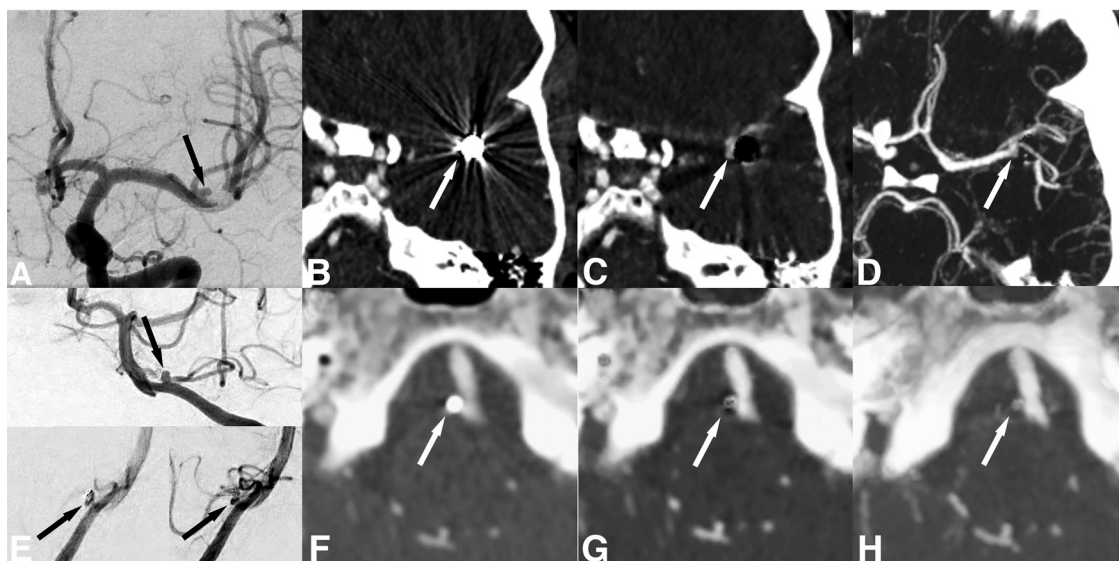


FIG 1. Example cases of residual aneurysms. A-D, Example case of a residual left middle cerebral artery bifurcation aneurysm after prior primary coil embolization. A, Single arterial phase anteroposterior cranial view on follow-up diagnostic cerebral angiogram demonstrates an aneurysm residual following coil compaction. B, Axial CCTA image at the level of the aneurysm neck. C, Axial IM-DECTA image at the level of the aneurysm neck. D, Axial MIP IM-DECTA image at the level of the aneurysm neck. Arrows indicate the location of the residual aneurysm. E-H, Example case of a residual left posterior inferior cerebellar artery aneurysm after prior primary coil embolization. E, Upper panel: arterial phase anteroposterior cranial view on follow-up diagnostic cerebral angiogram demonstrating small residual aneurysm inferior to the coil mass. Lower panel: early and midarterial phase lateral cranial views demonstrate the residual aneurysm inferior to the coil mass. F, Axial CCTA image at the level of the aneurysm neck. G, Axial IM-DECTA image at the level of the aneurysm neck demonstrating volume averaging between the artifactually “dark” inferior aspect of the coil mass and the small opacified residual aneurysm. H, Axial MIP IM-DECTA image at the level of the aneurysm neck effectively subtracting the coil mass to better delineate the small residual aneurysm.

DISCUSSION

In this study, we found that IM-DECTA is significantly more sensitive and specific than CCTA or monoenergetic DECTA reconstructions for the detection and characterization of residual aneurysms after endovascular coil embolization. Similarly, we found that quantitative and qualitative measures of beam-hardening artifact adjacent to the coil mass are significantly reduced by using IM reconstructions, and overall image quality was considered superior by both neuroradiologist and neurosurgery readers. Prior studies have examined various DECT reconstructions, including combinations of metal-artifact reduction software and virtual monoenergetic reconstructions to reduce coil and clip artifacts after endovascular and surgical aneurysm treatment, though results were markedly limited regarding reduction of coil-associated artifacts, particularly with large or densely packed aneurysms.^{5,6,15} However, to our knowledge, no study has yet evaluated the utility of IM-DECTA reconstructions for the detection and characterization of residual aneurysms after coil embolization.

The IM-DECTA technique presented here leverages a unique artifact of the vendor specific DECT reconstruction software for IM images. This software uses a subtraction technique for the material basis pair (iodine and water) of the iodine map series, wherein the relative attenuation attributed to water for a given voxel is subtracted to generate the IM-DECTA images. As all endovascular coils are primarily composed of platinum and the k-edge of platinum (78.4 keV) overlaps with the center of the attenuation range for iodine (k-edge 33.2 keV), there is a supraphysiologic spike in attenuation in the center of the reconstruction range between the high- and low-energy beam energies (Fig 2). As the attenuation spike related to the k-edge of platinum occurs in the physiologic iodine attenuation range and therefore the software reconstruction range, there is erroneous failure to decompose the platinum-associated voxels by using the selected iodine/water material basis pair. We hypothesize

that this error may occur either due to overwhelming metal attenuation beyond the standard HU reconstruction range for the software, or due to inappropriate categorization of platinum-related attenuation as iodine outside of the software limited attenuation range. The resultant IM images show complete subtraction of the platinum coil mass, seen as an absence of attenuation (Fig 1; Online Supplemental Data) or “coil void,” which is leveraged here to improve the contrast-to-noise ratio of the adjacent iodine opacified vessel and any associated residual aneurysms. The diagnostic utility of the platinum subtraction artifact on IM-DECTA images is further maximized with the generation of MIP images, as any MIP series with thickness greater than or equal to the maximum aneurysm diameter will result in complete subtraction of the coil void, leaving only the opacified parent vessel and any residual aneurysm visible (Fig 1).

Subtraction of the coil void further improves residual aneurysm conspicuity in a manner analogous to that seen on standard CTA MIP images in untreated patients without adjacent metallic hardware, allowing the blind-ending aneurysm to stand out against the otherwise linear branched vasculature. IM-DECTA and MIP IM-DECTA images are also therefore analogous to MRA images in the follow-up of patients with endovascularly treated aneurysms, wherein susceptibility artifact at the coil mass results in a signal void and only adjacent intravascular flow-related enhancement is visible. However, IM-DECTA theoretically carries benefits of speed of acquisition, superior spatial resolution and lower cost than MRA, but future studies to directly compare the extent of metal artifact against MRA are warranted, particularly as our findings suggest that very small residual aneurysms (<1.8 mm) or those with high coil-to-aneurysm size ratios (>5) may be more difficult to detect, despite being poorly powered for this sub-analysis. Accordingly, the IM-DECTA technique may act as a proof-of-concept demonstration for custom reconstruction parameters of multi-energetic CT, including DECT or photon-counting CT, to specifically decompose and subtract attenuation related to specific clip, stent, or intrasaccular flow disrupting device materials.

This study has multiple limitations. The small sample size and reliance on a reconstruction artifact limited to the software of a single DECT vendor limit generalizability and ease of testing of this technique at other institutions. Additionally, the long interval between DECTA and DSA for some patients introduces potential error if target aneurysms underwent evolution between the 2 studies, including growth or thrombosis. Our study is additionally underpowered to assess if aneurysm detection with DECTA is affected by adjacent osseous structures or tortuous vasculature given that most included aneurysms are >3 mm distant from

Table 4: Quantitative image noise assessment

	Mean HU	SD HU	SEM	P-Value
CCTA	445	103.2	13.3	
50-keV CTA	424	78.1	10.1	.06
70-keV CTA	765	129.6	16.7	.07
IM-DECTA	130	27.9	3.6	<.01
MIP IM-DECTA	160	26.8	3.5	<.01

Note:—Quantitative image noise assessment data as compared against reference CCTA, with the mean standard deviation HU values acquired by ROI placement within the parent vessel adjacent to each aneurysm neck used as a surrogate for beam-hardening artifact, with higher mean standard deviation values reflecting more extensive artifact.

Table 5: Qualitative image noise assessment and interpretability

	IQ1	IQ2	IQ3	Mode	κ	Neck Visualization
CCTA	14/25 (56%)	11/25 (44%)	0/25 (0%)	0	0.34	11/25 (44%)
50-keV CTA	3/25 (12%)	16/25 (64%)	6/25 (24%)	1	0.23	18/25 (72%)
70-keV CTA	5/25 (20%)	16/25 (64%)	4/25 (16%)	1	0.27	20/25 (80%)
IM-DECTA	0/25 (0%)	8/25 (32%)	17/25 (68%)	2	0.49	24/25 (96%)
MIP IM-DECTA	0/25 (0%)	6/25 (24%)	19/25 (76%)	2	0.58	24/25 (96%)

Note:—Qualitative image noise assessment based on Likert-style scale reader scores for each CTA series, with interreader agreement assessed by Cohen κ and reported neck visualization for each series. All series demonstrated a significant improvement in neck visualization over reference CCTA as assessed by the nonparametric Kruskal-Wallis test.

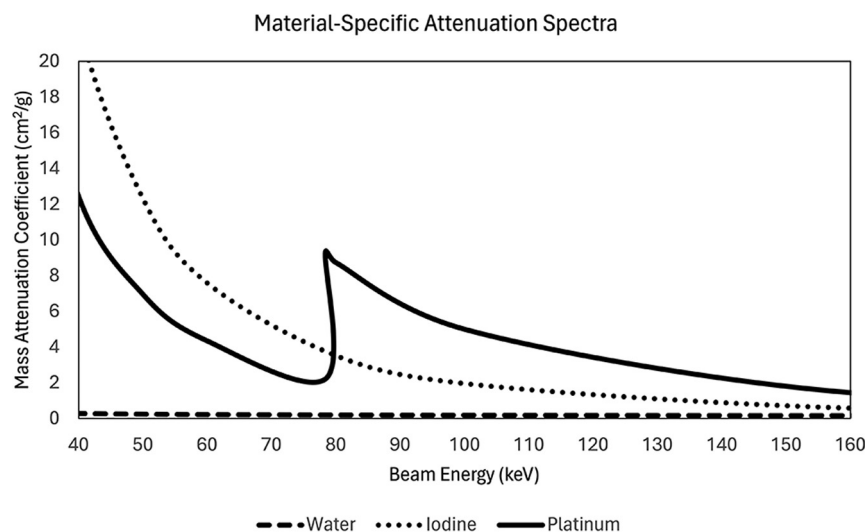


FIG 2. Metallic spectral analysis graph. Mass attenuation coefficients (cm^2/g) of the material basis pair used in iodine map reconstructions (iodine and water) and of platinum, plotted against beam energy (keV) within the CT imaging range. The energy spectrum of platinum demonstrates a k-edge at 78.4 keV with a resultant attenuation spike within the reconstruction range of the material basis pairs, resulting in artifactual subtraction by the reconstruction software. Spectral data acquired from the NIST Standard Reference Database 126; DOI: 10.18434/T4D01F.

the skull base, further limiting generalizability of these results to aneurysms at all locations. The lack of an MRA comparison in our study prevents direct comparison against a common and current standard-of-care for many institutions in the follow-up of previously endovascularly treated aneurysms but presents a target for future study.

CONCLUSIONS

IM-DECTA and MIP IM-DECTA leverages a unique reconstruction artifact to subtract platinum coil mass and is superior to CCTA and monoenergetic DECTA for the detection of residual aneurysms after endovascular coiling.

Disclosure forms provided by the authors are available with the full text and PDF of this article at www.ajnr.org.

REFERENCES

1. Wolman DN, Patel BP, Wintermark M, et al. **Dual-energy computed tomography applications in neurointervention.** *J Comput Assist Tomogr* 2018;42:831–39 [CrossRef Medline](#)
2. McCollough CH, Boedeker K, Cody D, et al. **Principles and applications of multi-energy CT report of AAPM task group 291.** *Med Phys* 2020;47:e881–e912 [CrossRef Medline](#)
3. Lavoie P, Gariépy J-L, Milot G, et al. **Residual flow after cerebral aneurysm coil occlusion: diagnostic accuracy of MR angiography.** *Stroke* 2012;43:740–46 [CrossRef Medline](#)
4. Kaufmann TJ, Huston J III, Mandrekar JN, et al. **Complications of diagnostic cerebral angiography: evaluation of 19,826 consecutive patients.** *Radiology* 2007;243:812–19 [CrossRef Medline](#)
5. Mellander H, Fransson V, Ydström K, et al. **Metal artifact reduction by virtual monoenergetic reconstructions from spectral brain CT.** *Eur J Radiology Open* 2023;10:100479 [CrossRef Medline](#)
6. Mocanu I, Van Wettere M, Absil J, et al. **Value of dual-energy CT angiography in patients with treated intracranial aneurysms.** *Neuroradiology* 2018;60:1287–95 [CrossRef Medline](#)
7. Zaeske C, Hickethier T, Borggrefe J, et al. **Postinterventional assessment after stent and flow-diverter implantation using CT: influence of spectral image reconstructions and different device types.** *AJNR Am J Neuroradiol* 2021;42:516–23 [CrossRef Medline](#)
8. Patino M, Prochowski A, Agrawal MD, et al. **Material separation using dual-energy CT: current and emerging applications.** *Radiographics* 2016;36:1087–105 [CrossRef Medline](#)
9. McCollough CH, Leng S, Yu L, et al. **Dual- and multi-energy CT: principles, technical approaches, and clinical applications.** *Radiology* 2015;276:637–53 [CrossRef Medline](#)
10. Bahner ML, Bengel A, Brix G, et al. **Improved vascular opacification in cerebral computed tomography angiography with 80 kVp.** *Invest Radiology* 2005;40:229–34 [CrossRef Medline](#)
11. Schneider D, Apfalter P, Sudarski S, et al. **Optimization of kiloelectron volt settings in cerebral and cervical dual-energy CT angiography determined with virtual monoenergetic imaging.** *Acad Radiology* 2014;21:431–36 [CrossRef Medline](#)
12. Zhang X, Pan T, Lu SS, et al. **Application of monochromatic imaging and metal artifact reduction software in computed tomography angiography after treatment of cerebral aneurysms.** *J Comput Assist Tomogr* 2019;43:948–52 [CrossRef Medline](#)
13. Stapleton CJ, Torok CM, Rabinov JD, et al. **Validation of the Modified Raymond-Roy classification for intracranial aneurysms treated with coil embolization.** *J Neurointerv Surg* 2016;8:927–33 [CrossRef Medline](#)
14. Verdun FR, Racine D, Ott JG, et al. **Image quality in CT: From physical measurements to model observers.** *Phys Med* 2015;31:823–43 [CrossRef Medline](#)
15. Winklhofer S, Hinzpeter R, Stocker D, et al. **Combining monoenergetic extrapolations from dual-energy CT with iterative reconstructions: reduction of coil and clip artifacts from intracranial aneurysm therapy.** *Neuroradiology* 2018;60:281–91 [CrossRef Medline](#)